

RADIATION INTERFEROMETRY

PACS numbers: 07.60.Vg; 07.60.Ly; 42.55.Px; 42.60.Mi
DOI: 10.1070/QE2013v043n10ABEH015174

Noise power spectral density of a fibre scattered-light interferometer with a semiconductor laser source

A.E. Alekseev, V.T. Potapov

Abstract. **Spectral characteristics of the noise intensity fluctuations at the output of a scattered-light interferometer, caused by phase fluctuations of semiconductor laser radiation are considered. This kind of noise is one of the main factors limiting sensitivity of interferometric sensors. For the first time, to our knowledge, the expression is obtained for the average noise power spectral density at the interferometer output versus the degree of a light source coherence and length of the scattering segment. Also, the approximate expressions are considered which determine the power spectral density in the low-frequency range (up to 200 kHz) and in the limiting case of extended scattering segments. The expression obtained for the noise power spectral density agrees with experimental normalised power spectra with a high accuracy.**

Keywords: *scattered radiation, semiconductor laser, noise power spectral density, backscattered light interferometer.*

1. Introduction

The problem of determining the noise spectral characteristic of a fibre scattered-light interferometer arises in studying the interferometer sensitivity to external phase influence. In addition, consideration of the noise power spectrum of the scattered-light interferometer with a cw radiation source is a first step to studying noise of the coherent reflectometer, in which cw laser radiation is modulated by short-duration pulses [1, 2].

In the present work, one of the main kinds of noise in an interferometer with a cw radiation source, originating from random phase fluctuations of the source field, is investigated. The phase noise of the source is converted in the interferometer to output intensity fluctuations similarly to classical Michelson and Mach–Zehnder interferometer schemes [3, 4]. However, in contrast to interferometers with two interfering rays, in a scattered-light interferometer a multipath interference occurs of the random fields scattered by a large number of scattering centres distributed within a considered segment. In such an interferometer, the phase delay between interfering fields always exists, whose maximal value increases with the length of the scattering segment.

A.E. Alekseev IRE-Polus Research and Technology Association, pl. Vvedenskogo 1, 141190 Fryazino, Moscow region, Russia; e-mail: aleksey.e.alekseev@gmail.com;
V.T. Potapov V.A. Kotel'nikov Institute of Radio Engineering and Electronics (Fryazino Branch), Russian Academy of Sciences, pl. Vvedenskogo 1, 141190 Fryazino, Moscow region, Russia

Received 12 March 2013; revision received 18 June 2013
Kvantovaya Elektronika **43** (10) 968–973 (2013)
Translated by N.A. Raspopov

Thus, the base configuration of the interferometer in question is a single scattering segment, which can be realised, for example, with a waveguide circulator (Fig. 1). A main specific feature of a scattered-light interferometer is that all the fields involved in the interference have random amplitudes and phases, which vary in time under the action of environment. As a result, the average intensity of the scattered radiation at the interferometer output undergoes temporal fluctuations or random drift, whose statistical behaviour is considered in [5–7].

In addition to fluctuations of average intensity, noise fluctuations are also observed, with the noise power randomly varying in time. The presence of these fluctuations is one of the factors limiting the sensitivity of the external-action sensor on the basis of a scattered-light interferometer [8, 9]. The aim of the present work is to study the spectral properties of output noise intensity fluctuations of the scattered-light interferometer, caused by phase fluctuations of the field of the laser source operating in cw mode.

2. Theoretical part

Consider the two main schemes of a scattered-light interferometer: with a single (Fig. 1) and two (Fig. 2) scattering segments. The first scheme is basic one, whereas the second scheme provides obtaining the interference of rays, scattered by two independent segments. Features of the second scheme, methods for demodulation of the scattered radiation and detection of external phase action on the fibre are described in our previous publications [8, 9]. The spectral characteristics of noise for both schemes under the conditions reported below are identical; however, experimental verification of the second scheme is simpler. Note that a necessary element providing the possibility of correct measurements in the second scheme is the acousto-optical modulator that shifts the radia-

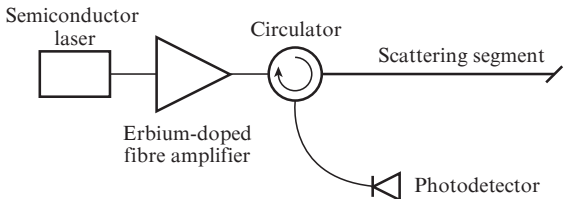

Figure 1. Basic configuration of the scattered-light interferometer. Radiation of the semiconductor laser source is amplified and passes through a circulator to a scattering segment; radiation scattered by the segment is coupled out through the same circulator and directed to a wideband photodetector.

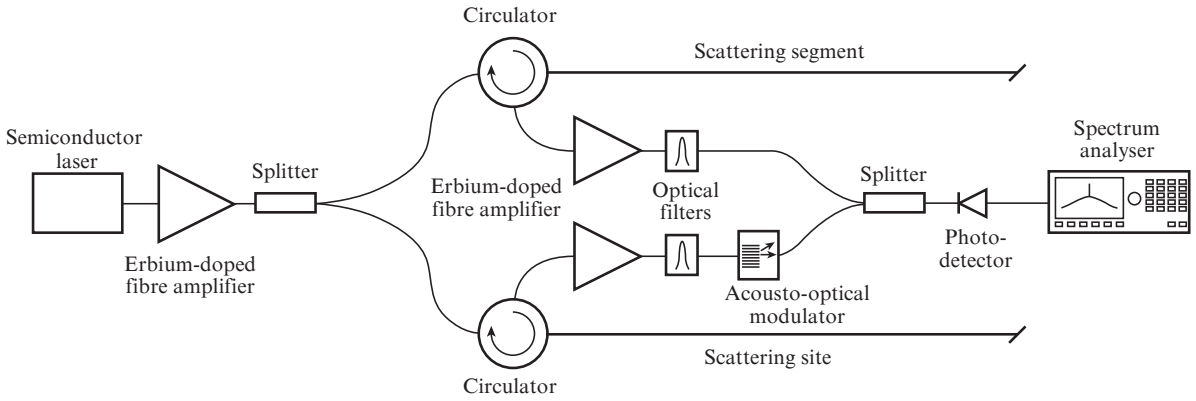

Figure 2. Experimental setup: scattered-light interferometer with two scattering segments.

tion frequency in one interferometer arm by the known value $f_0 = 200$ MHz.

The noise power spectral density of intensity fluctuations arising in a scattered-light interferometer can be found by using the Wiener–Khintchine theorem [10], according to which, for the wide-sense stationary processes, the autocorrelation function and the power spectral density are the Fourier transforms of each other, respectively.

Consider a radiation scattering process in an isotropic optical fibre. The scattering medium will be considered by using the earlier model [5–7, 11], in which the scattering centres are uniformly distributed over a volume of the fibre of length L much longer than the radial dimension of the medium. The dimension of each scattering centre is much less than the radiation wavelength, and the scattering amplitudes for centres are uncorrelated circular complex Gaussian random variables [10, 11], for which the following expressions are valid

$$\langle \rho^*(z_n)\rho(z_m)\rangle_\rho = \rho_0 \delta(z_n - z_m), \tag{1}$$

$$\langle \rho(z_n)\rho(z_m)\rangle_\rho = 0, \tag{2}$$

where $\rho(z_n)$ and $\rho(z_m)$ are the differential amplitude coefficients of Rayleigh scattering, i.e., the coefficients of scattering for the infinitesimal small fibre sections with coordinates z_n and z_m ($m,n = 1,...,N$); $\langle ... \rangle_\rho$ is averaging over an ensemble of all possible realisations $\{\rho\}$; $\rho_0/2$ is the dispersion of the real and imaginary parts of the scattering coefficient; and δ is the delta function.

Consider the base scheme of a scattered-light interferometer (Fig. 1). The analytical representation for the source electric field vector at the input into a scattering fibre can be written in the form

$$\boldsymbol{U}_s(t) = \boldsymbol{A}_s(t)\exp(i\omega_0 t),\ \ \boldsymbol{A}_s(t) = \boldsymbol{p}_s\sqrt{I_s}\exp[i\varphi_s(t)], \tag{3}$$

where $\boldsymbol{A}_s(t)$ is the vector of the complex amplitude of the source field; $\boldsymbol{p}_s$ is the polarisation vector; I_s is the source radiation intensity; $\varphi_s(t)$ is the phase of source radiation; and ω_0 is the optical frequency.

For simplicity we will assume that the polarisation state is constant over the considered segment, and so is the intensity of laser radiation. Then for the first interferometer scheme (Fig. 1), the complex amplitude of scattered radiation at the input for a certain realisation of the scattering coefficient distribution $\{\rho\} = \{\rho(z_1), \rho(z_2), ..., \rho(z_N)\}$, has the form [11]

$$A^{(\rho)}_{scat1} = \int_0^L A_s(t - 2z/v_{gr})\exp(-\alpha z/2)\exp(-2ikz)\rho(z)\,dz, \tag{4}$$

where α is the linear intensity attenuation coefficient in the fibre of length L; k is the radiation propagation constant; v_{gr} is the radiation group velocity; and index ρ means that the parameter refers to a single fixed realisation of the scattering coefficient distribution. We assume that within the limits of the considered segment in a fibre, the complex amplitude of the radiation field weakly damps, i.e., the coefficient α is sufficiently small (which is true for a standard single-mode fibre SMF-28 at the wavelengths near 1555 nm, $\alpha = 0.2$ dB km^{-1}). The instantaneous radiation intensity, scattered by the fibre segment is, according to (4)

$$I^{(\rho)}_{scat1} = \int_0^L \int_0^L A_s^*(t - 2z_1/v_{gr})A_s(t - 2z_2/v_{gr}) \times \exp(2ikz_1)\exp(-2ikz_2)\rho^*(z_1)\rho(z_2)\,dz_1\,dz_2. \tag{5}$$

In view of the fact that the phase of the source field $A_s(t)$ varies randomly, the instantaneous intensity (5) undergoes noise fluctuations near an average value. In addition, if the particular realisation of scattering coefficient distribution $\{\rho\}$ varies, then the average intensity (5) also changes. The power spectral density of intensity fluctuations of scattered radiation for a particular fixed realisation of the scattering coefficient distribution $\{\rho\}$ can be obtained from the Fourier transform of the autocorrelation or autocovariance intensity function (5) [3, 4, 11]. Write out the expressions for the autocorrelation and autocovariance functions of instantaneous intensity (5) for the particular realisation $\{\rho\}$:

$$R^{(\rho)}_{scat1}(t, t+\tau) = \langle I^{(\rho)}_{scat1}(t) I^{(\rho)}_{scat1}(t+\tau)\rangle_t, \tag{6}$$

$$C^{(\rho)}_{scat1}(t, t+\tau) = \langle I^{(\rho)}_{scat1}(t) I^{(\rho)}_{scat1}(t+\tau)\rangle_t - \langle I^{(\rho)}_{scat1}(t)\rangle_t \langle I^{(\rho)}_{scat1}(t+\tau)\rangle_t, \tag{7}$$

where $\langle ... \rangle_t$ means averaging over time. Under real physical conditions, static realisation of the scattering coefficient distribution $\{\rho\}$ is not fixed, it varies under the action of environment: the mutual positions of scattering centres and phases of the scattered fields vary, which leads to changes in both the average intensity and its noise characteristics. In practice it is useful to know the average noise level at the interferometer output, i.e., the noise power spectral density for scattered radiation averaged over all possible statistically

equivalent distributions of scattering coefficients $\{\rho\}$ or over all possible statistically equivalent scattering segments. For calculating this parameter we take an average of the autrocorrelation function (6) over all possible realisations $\{\rho\}$:

$$R_{\text{scat1}}(t,t+\tau) = \langle R^{(\rho)}_{\text{scat1}}(t,t+\tau)\rangle_\rho = \langle\langle I^{(\rho)}_{\text{scat1}}(t) I^{(\rho)}_{\text{scat1}}(t+\tau)\rangle_t\rangle_\rho. \quad (8)$$

In expression (8), averaging over time and over ensemble can be performed independently because the scattering amplitude and complex source field amplitude are independent of each other. In making averaging in (8) one should employ the Gaussian moment theorem for complex random variables [12], which in view of (1) yields the expression for the 4th moment

$$\langle\rho^*(z_1)\rho(z_2)\rho^*(z_3)\rho(z_4)\rangle_\rho = \rho_0^2\delta(z_1-z_2)\,\delta(z_3-z_4) + \rho_0^2\delta(z_2-z_3)\,\delta(z_1-z_4). \quad (9)$$

The resulting expression for correlation function (8) averaged over the ensemble reduces to

$$R_{\text{scat1}}(t,t+\tau) = \rho_0^2\int_0^L\int_0^L I_s^2\,\mathrm{d}z_1\mathrm{d}z_3 + \rho_0^2\int_0^L\int_0^L\langle A_s^*(t-2z_1/v_{gr})A_s(t-2z_2/v_{\text{gr}}) \times A_s^*(t+\tau-2z_2/v_{\text{gr}})A_s(t+\tau-2z_1/v_{\text{gr}})\rangle_t\,\mathrm{d}z_1\mathrm{d}z_2. \quad (10)$$

The first summand in (10) is the square of the intensity averaged over ensemble $\{\rho\}$ for the radiation scattered by a single segment of length L, which, according to (5) and (1) is defined by the expression [11]

$$I^{\text{m}}_{\text{scat1}} = \langle I^{(\rho)}_{\text{scat1}}(t)\rangle_\rho = \rho_0\int_0^L I_s\mathrm{d}z = \frac{v_{\text{gr}}}{2}\rho_0 I_s T, \quad (11)$$

where $T = 2L/v_{\text{gr}}$. The second summand is the double integral of the 4th moment for the source field $A_s(t)$, which can be transformed taking into account that the phase of semiconductor laser radiation $\varphi_s(t)$ varies according to the random walk statistics [6, 7, 13]. By performing the averaging of the integrand in (10) over time as in [3, 4] and making a substitution $\tau_1 = 2z_1/v_{\text{gr}}$, $\tau_2 = 2z_2/v_{\text{gr}}$ we obtain the expression for the autocorrelation function of scattered radiation intensity averaged over ensemble $\{\rho\}$, which is independent of time t:

$$R_{\text{scat1}}(\tau) = \frac{v_{\text{gr}}^2}{4}\rho_0^2\int_0^T\int_0^T I_s^2\,\mathrm{d}\tau_1\mathrm{d}\tau_2 + \frac{v_{\text{gr}}^2}{4}\rho_0^2\int_0^T\int_0^T I_s^2\exp\Big(-\frac{2\,|\tau_2-\tau_1|}{\tau_{\text{coh}}}\Big)\mathrm{d}\tau_1\mathrm{d}\tau_2 + \frac{v_{\text{gr}}^2}{4}\rho_0^2\int_0^T\int_0^T I_s^2\Big[\exp\Big(-\frac{2\,|\tau|}{\tau_{\text{coh}}}\Big) - \exp\Big(-\frac{2\,|\tau_2-\tau_1|}{\tau_{\text{coh}}}\Big)\Big] \times\Pi\Big(\frac{\tau}{2\,|\tau_2-\tau_1|}\Big)\mathrm{d}\tau_1\mathrm{d}\tau_2, \quad (12)$$

where $|\tau_2-\tau_1|$ is the time delay between the interfering fields; $\tau_{\text{coh}} = 1/(\pi\Delta\nu)$ is the coherence time for the radiation source; $\Delta\nu$ is the spectral bandwidth of the radiation source; and the rectangular function Π is determined by the expression

$$\Pi\Big(\frac{\tau}{2\,|\tau_2-\tau_1|}\Big) = \begin{cases}1, & |\tau| \leqslant |\tau_2-\tau_1|,\\ 0, & |\tau| > |\tau_2-\tau_1|.\end{cases} \quad (13)$$

Similarly, the product of the time-averaged intensities is averaged over ensemble $\{\rho\}$:

$$\langle\langle I^{(\rho)}_{\text{scat1}}(t)\rangle_t\langle I^{(\rho)}_{\text{scat1}}(t+\tau)\rangle_t\rangle_\rho = \frac{v_{\text{gr}}^2}{4}\rho_0^2\int_0^T\int_0^T I_s^2\,\mathrm{d}\tau_1\mathrm{d}\tau_2 + \frac{v_{\text{gr}}^2}{4}\rho_0^2\int_0^T\int_0^T I_s^2\exp\Big(-\frac{2\,|\tau_2-\tau_1|}{\tau_{\text{coh}}}\Big)\mathrm{d}\tau_1\mathrm{d}\tau_2. \quad (14)$$

By subtracting (14) from (12) we obtain the expression for the intensity autocovariance function of the scattered-light interferometer with a single scattering segment of length L, which is averaged over all possible distributions of scattering coefficients:

$$C_{\text{scat1}}(\tau) = \frac{(I^{\text{m}}_{\text{scat1}})^2}{T^2}\int_0^T\int_0^T\Big[\exp\Big(-\frac{2\,|\tau|}{\tau_{\text{coh}}}\Big) - \exp\Big(-\frac{2\,|\tau_2-\tau_1|}{\tau_{\text{coh}}}\Big)\Big] \times\Pi\Big(\frac{\tau}{2\,|\tau_2-\tau_1|}\Big)\mathrm{d}\tau_1\mathrm{d}\tau_2. \quad (15)$$

Expression (15) has the relatively simple physical meaning, that can be elucidated by considering the known intensity autocovariance function of a Mach–Zehnder or Michelson interferometer [3, 4, 13, 14], which can be presented in the form [4]

$$C_{\text{MZ}}(\tau) = \frac{I_{\text{MZ}}^2}{2}\Big\{\exp\Big(-\frac{2\,|\tau|}{\tau_{\text{coh}}}\Big) - \exp\Big(-\frac{2\,|\tau_2-\tau_1|}{\tau_{\text{coh}}}\Big) + \Big[\exp\Big(-\frac{4\,|\tau_2-\tau_1|-2\,|\tau|}{\tau_{\text{coh}}}\Big) - \exp\Big(-\frac{2\,|\tau_2-\tau_1|}{\tau_{\text{coh}}}\Big)\Big]\cos 2\varphi\Big\} \times\Pi\Big(\frac{\tau}{2\,|\tau_2-\tau_1|}\Big), \quad (16)$$

where $\varphi = k(z_2-z_1)$ is the optical path difference in the interferometer and I_{MZ} is the average intensity of radiation at the interferometer output. A Mach–Zehnder or Michelson interferometer has a minimal or maximal transmission at $\cos\varphi = \pm 1$ ($\varphi = \pi l$, where l is an integer) and it is usually said that the interferometer operating point is outside quadrature. On the contrary, at $\cos\varphi = 0$ ($\varphi = \pi/2 + \pi l$) the transmission of interferometer corresponds to the intensity I_{MZ} and it is usually said that the interferometer operating point resides in quadrature [4, 14]. For the in-quadrature and out-off-quadrature operation regimes the interferometer output noise differs. Note that if expression (16) is averaged over all values of the operating point φ, then the second summand in (16) vanishes and (16) will correspond to the integrand in (15) within the accuracy of a constant factor. Thus, one may assume that the intensity autocovariance function averaged over ensemble $\{\rho\}$ for the scattered-light interferometer (15) is the sum of the autocovariance functions for all possible elementary interferometers formed by the scattering centres with the field time delays $0 \leqslant |\tau_1 - \tau_2| \leqslant T$, which are averaged over all positions of their operating points φ. In view of the linearity of the Fourier

transform, the power spectral density averaged over ensemble $\{\rho\}$ for the scattered-light interferometer is the sum of the power spectral densities averaged over all positions of operating points for all elementary Michelson interferometers formed by the scattering centres.

In the case of a scattered-light interferometer with two scattering segments (Fig. 2), the more labourious calculation, which includes averaging of 16 terms of autocorrelation function and 16 terms of intensity products over ensemble, finally results in the following expression for the averaged autocovariance function:

$$C_{\text{scat2}}(\tau) = 2\frac{(I^{\text{m}}_{\text{scat1}})^2}{T^2}\Big[2\int_0^T\int_0^T F(\tau,\tau_1,\tau_2)\,\mathrm{d}\tau_1\mathrm{d}\tau_2 + \exp(2\pi\mathrm{i}f_0\tau)\int_0^T\int_{T_0}^{T+T_0} F(\tau,\tau_1,\tau_2')\,\mathrm{d}\tau_1\mathrm{d}\tau_2' + \exp(-2\pi\mathrm{i}f_0\tau)\int_{T_0}^{T+T_0}\int_0^T F(\tau,\tau_1',\tau_2)\,\mathrm{d}\tau_1'\mathrm{d}\tau_2\Big], \quad (17)$$

where

$$F(\tau,\tau_1,\tau_2) = \Big[\exp\Big(-\frac{2|\tau|}{\tau_{\text{coh}}}\Big) - \exp\Big(-\frac{2|\tau_2-\tau_1|}{\tau_{\text{coh}}}\Big)\Big]\Pi\Big(\frac{\tau}{2|\tau_2-\tau_1|}\Big);$$

f_0 is the frequency of the acousto-optical modulator and T_0 is the additional delay of fields in the interferometer. The first summand in (17), which is similar to expression (15), is responsible for the sum of the autocovariance functions of intensities of the fields scattered independently by the first and second scattering segments of the interferometer. The second and third summands correspond to the cross-autocovariance functions for the first and second scattering segments of the interferometer, i.e., similarly to (15), in expression (17) the autocovariance functions are summed over all possible interferometers formed by the scattering centres, but for the two segments in this particular case.

An important particular case is the additional time delay of fields equal to zero ($T_0 = 0$), i.e., the case, where the interferometer with two scattering segments is balanced. Then, expression (17) may be represented in terms of expression (15):

$$C_{\text{scat2}}(\tau) = 2C_{\text{scat1}}(\tau) + \exp(2\pi\mathrm{i}f_0\tau)C_{\text{scat1}}(\tau) + \exp(-2\pi\mathrm{i}f_0\tau)C_{\text{scat1}}(\tau). \quad (18)$$

Thus, the autocovariance function for the interferometer corresponding to the second scheme (Fig. 2) is distinct from that for the interferometer corresponding to the first scheme (Fig. 1) by two additional copies of the autocovariance function (15) with the phase factors only differing in the phase sign. Due to the linearity of the Fourier transform, the spectral characteristic for the second scheme obtained from (18) differs from that for the first scheme obtained from (15) by two additional spectrum copies for the first scheme shifted by frequency f_0 to positive and negative ranges. In this case, the spectral component at frequency f_0 can be easy measured experimentally.

By performing labourious Fourier transformation of expression (15) and double integration with the relationships for the spectral characteristics of the Mach–Zehnder interferometer taken into account [4] we obtain the expression for the noise power spectral density, determined by averaged autocovariance function (15):

$$S_{\text{scat1}}(f) = \frac{2(I^{\text{m}}_{\text{scat1}})^2}{T^2}\frac{\tau_{\text{coh}}}{1+(\pi f\tau_{\text{coh}})^2}\Big(\frac{T^2}{2} + \frac{4}{\tau_{\text{coh}}} \times \frac{\tau_{\text{coh}}^4}{[4+(2\pi f\tau_{\text{coh}})^2]^2}\Big\{\exp\Big(-\frac{2T}{\tau_{\text{coh}}}\Big)\Big[-\frac{2}{\tau_{\text{coh}}}\cos(2\pi fT) + 2\pi f\sin(2\pi fT)\Big] + \frac{2}{\tau_{\text{coh}}}\Big\} + \Big(2\pi f - \frac{2}{\pi f\tau_{\text{coh}}^2}\Big) \times \frac{\tau_{\text{coh}}^4}{[4+(2\pi f\tau_{\text{coh}})^2]^2}\Big\{\exp\Big(-\frac{2T}{\tau_{\text{coh}}}\Big)\Big[\frac{2}{\tau_{\text{coh}}}\sin(2\pi fT) + 2\pi f\cos(2\pi fT)\Big] - 2\pi f\Big\} - \frac{4T}{\tau_{\text{coh}}}\frac{\tau_{\text{coh}}^2}{4+(2\pi f\tau_{\text{coh}})^2}\Big). \quad (19)$$

The expression for the noise power spectral density in the case of the scheme with two scattering segments observed at frequency f_0 has, according to (18), a similar form. If the autocorrelation function (12) is used for the calculation, then the spectrum will comprise additional components – δ-functions at a zero frequency with the amplitudes determined by (14); one may show that similar components at the frequencies $\pm f_0$ will also arise in the spectral characteristic of the interferometer with two scattering segments.

The power spectral densities (19) for the sources with the spectral widths of 2 and 500 kHz normalised to square average intensity of scattered radiation are shown in Fig. 3. The dependences look similar though the dependence for the laser with less coherence is more sloping. One can see that in the frequency range up to 200 kHz (which includes the acoustic frequency band) the power spectral densities for the two sources exhibit weak frequency dependence. Hence, in this range each of the spectral characteristics can be approximated by a constant value of the power spectral density, i.e., by white noise. Expanding expression (19) in series near zero frequency and only retaining zero-order terms we obtain the relationship

$$S_{\text{scat1}}(f) \approx \frac{2(I^{\text{m}}_{\text{scat1}})^2}{T^2}\tau_{\text{coh}}\Big[\frac{T^2}{2} + \frac{3\tau_{\text{coh}}^2}{4} - T\tau_{\text{coh}}$$

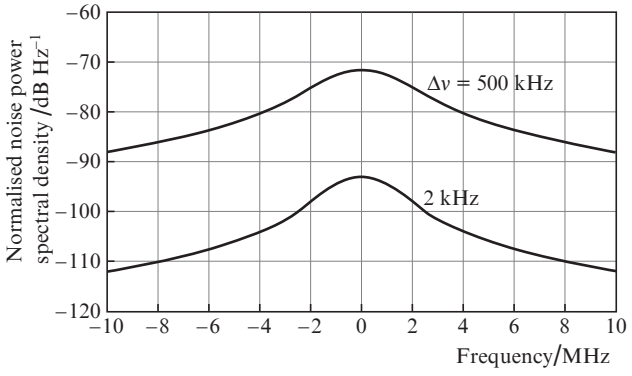

Figure 3. Theoretical average noise power spectral density at the output of the scattered-light interferometer for the lasers with spectral widths $\Delta\nu$ = 2 and 500 kHz and with scattering segment length of 50 m.

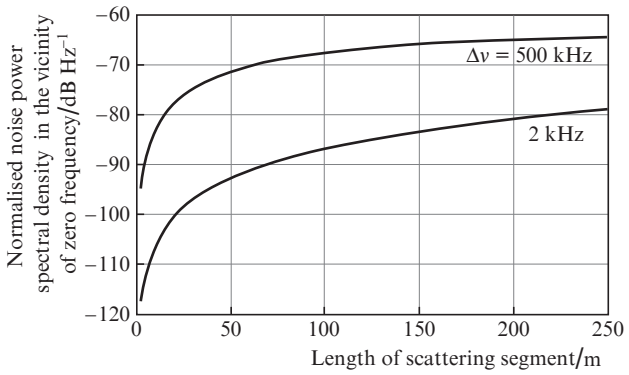

Figure 4. Theoretical average noise power spectral density for the scattered-light interferometer in the vicinity of zero frequency vs. length of scattering segment in the cases of laser spectral width $\Delta\nu$ = 2 and 500 kHz. For the segment of length 50 m, the average noise levels at the interferometer output for the two lasers differ by 21 dB.

$$- \exp\left(-\frac{2T}{\tau_{\rm coh}}\right)\left(\frac{3\tau_{\rm coh}^2}{4} + \frac{T\tau_{\rm coh}}{2}\right)\Bigg]. \qquad (20)$$

It is easy to verify by a direct substitution that at the frequency of 200 kHz the relative difference in the power densities calculated by formulae (19) and (20) is less than 1%. The dependence of $S_{\rm scat1}(f)$ (20) on the length of scattering segment $L = Tv_{\rm gr}/2$ for lasers with different degrees of coherence is shown in Fig. 4. For lengths $L > 10$ m, the relative difference of noise power for the two lasers monotonically falls reaching zero value at $L = 1750$ m; for the scattering segment with $L = 50$ m it is 21 dB. Finally, note that at lengths of scattering segments much longer than the source coherence length, that is, at $T \gg \tau_{\rm coh}$ under the assumption that the propagating radiation weakly attenuates along the scattering segment, expression (19) is simplified and takes the form

$$S_{\rm scat1}(f) \approx (I^{\rm m}_{\rm scat1})^2 \frac{\tau_{\rm coh}}{1 + (\pi f \tau_{\rm coh})^2}, \qquad (21)$$

here, one can see that the spectral characteristic is of Lorentzian type with the full width at half maximum equal to the double spectral width of source emission $2\Delta\nu$.This limiting case agrees with the results of [11] and holds for semiconductor sources with a low degree of coherence.

3. Experimental part

In order to confirm the theoretical results, the experimental setup was designed, which corresponds to Fig. 2. Radiation of a semiconductor laser operating in cw mode at the wavelength near 1555 nm was amplified by an erbium-doped fibre amplifier to a power of 25 dBm. After the 50% splitter, the radiation beams passed through circulators into two scattering segments, which were presented by pieces of a single-mode fibre SMF-28. The radiation scattered in each segment was coupled out through the same circulators and amplified by erbium-doped fibre pre-amplifiers. After filtration by the optical filters with the spectral bandwidths of 100 GHz, the radiation propagating in one interferometer arm passed through the acousto-optical modulator which shifted the radiation frequency by $f_0 = 200$ MHz.

The interference signal detected by a wide-band photodetector was then analysed by an Agilent E4411B spectrum analyser. The additional optical paths covered by the radiation in two interferometer arms from the output coupler to input into the scattering segment and from output of scattering segments to the photodetector (with the allowance made for the length of the amplifying fibre in the pre-amplifiers) were chosen with equal lengths. The lengths of the scattering segments varied from 50 to 90 m, remaining equal. To avoid reflection from the end of the scattering segment, the optical radiation was coupled out through knots of small radius at the end of the segments. Two laser types were employed: a high-coherence laser with the spectral bandwidth $\Delta\nu$ = 2 kHz and a standard telecommunication laser with $\Delta\nu$ = 500 kHz. For recording the statistically average power spectrum, the spectral analyser operated in the regime of averaging over 500 samples and the scanning was performed with resolution Δf = 10 kHz.

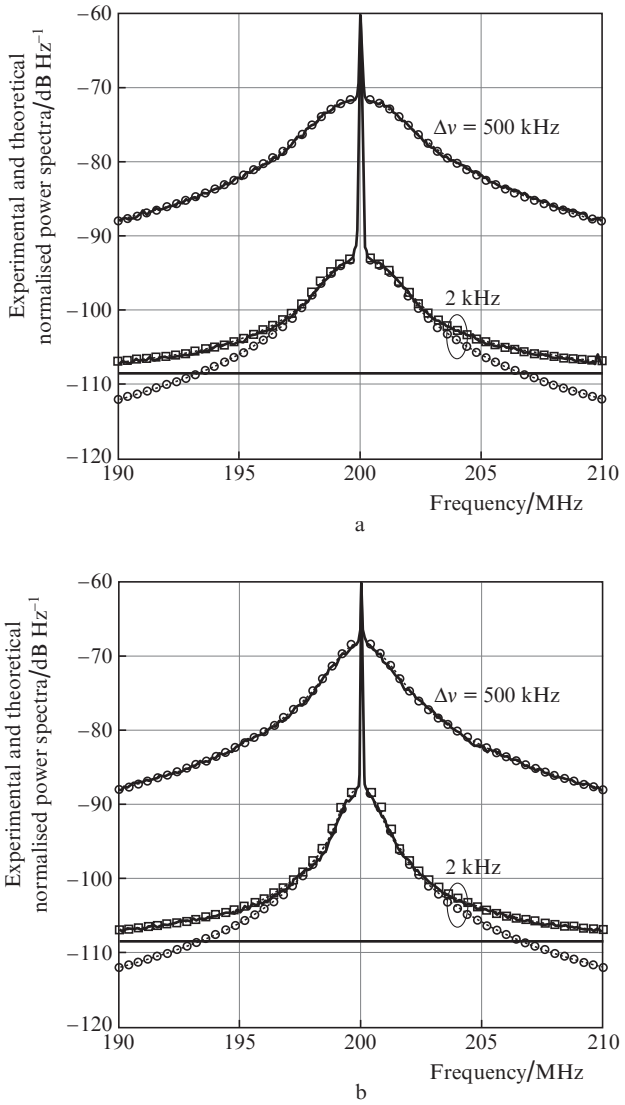

Figure 5. Normalised noise power spectra at the output of the scattered-light interferometer with the lengths of scattering segments (a) 50 and (b) 90 m each with the laser spectral width $\Delta\nu$ = 2 and 500 kHz. Solid curves refer to experimental noise power spectra averaged over 500 realisations (specrum analyser resolution is 10 kHz, and its video bandwidth is 10 kHz); circles denote the theoretical noise power spectra and squares denote theoretical noise power spectra with the noise of pre-amplifier and of photodetector taken into account. Solid horizontal lines mark a level of the noise due to pre-amplifiers and photodetector.

Theoretical and experimental power spectra normalised to the average value of scattered radiation power are presented in Fig. 5b for the two described laser types at the lengths of scattering segments $L = 50$ m each. One can see that at longer scattering segments the spectral characteristics become more abrupt. The peaks at the frequency of 200 MHz correspond to a harmonic component of the autocorrelation function. Similar experimental dependences were observed near zero frequency both for interferometers with one and two scattering segments. Solid curves refer to experimental power spectra of scattered radiation and circles denote the power spectra calculated by (19) for the spectral bandwidth of 10 kHz. For a low-coherence laser the curves coincide to a high degree of accuracy. However, for a high-coherence laser good agreement is only observed if the frequencies differ from the centre frequency by at most 2 MHz. In our opinion, such a behaviour is explained by the fact that the spectral components at high frequencies have a low power and an influence becomes noticeable of the noise produced by beatings of the signal with a spontaneous emission of the optical pre-amplifier and by shot and thermal noise of the photodetector. All the kinds of noise mentioned have a uniform distribution over spectrum in the range of measurements [15]. In our experimental setup the total normalised noise of all kinds was –109 dB Hz^{-1} (in Fig. 5 it is marked by a horizontal line). The spectra of scattered radiation power with this noise taken into account are marked in Fig. 5 by squares. Thus, with the additional noise of spontaneous emission and of the photodetector taken into account the theoretical and experimental spectral characteristics of scattered radiation coincide with high accuracy.

4. Conclusions

In the present work, spectral noise characteristics are considered for a fibre scattered-light interferometer with a semiconductor laser source. To our knowledge, for the first time the expression for the average noise power sepctral density of fluctuations at the interferometer output caused by phase fluctuations of the radiation source is derived. The power of noise intensity fluctuations depends on the degree of coherence of the laser source and on the length of the scattering segment in the interferometer. In a low-frequency range (up to 200 kHz) the noise power spectral density is well approximated by white noise, whose spectral density can be calculated by formula (20). Experimental normalised spectra coincide with the theoretical spectra to a high accuracy. Nevertheless, for the laser with a high degree of coherence in the frequency range where the noise power spectral density is low one should take into account the noise of optical preamplifier and of photodetector. The expressions obtained after normalising to the square average intensity of scattered radiation experimentally measured for a particular fibre can be employed for estimating the sensitivity and minimal detectable signal level while using a scattered-light interferometer as a sensor of external phase actions.

Acknowledgements. Authors are grateful to Ya.A. Tezadov for providing a laser source, photodetector and acousto-optical modulator.

References

1. Gorshkov B.G., Paramonov V.M., Kurkov A.S., Kulakov A.T., Zazirnyi M.V. *Kvantovaya Elektron.*, **36**, 963 (2006) [*Quantum Electron.*, **36**, 963 (2006)].
2. Nesterov E.T., Treshchikov V.N., Ozerov A.Zh., Sleptsov M.A., Kamynin V.A., Nanii O.E., Sus'yan A.A. *Pis'ma Zh. Tekh. Fiz.*, **37** (9), 55 (2011).
3. Petermann K., Weidel E. *IEEE J. Quantum Electron.*, **17** (7), 1251 (1981).
4. Moslehi B. *J. Lightwave Technol.*, **4** (11), 1704 (1986).
5. Alekseev A.E., Tezadov Ya.A., Potapov V.T. *Pis'ma Zh. Tekh. Fiz.*, **38** (2), 74 (2012).
6. Alekseev A.E., Tezadov Ya.A., Potapov V.T. *Radiotekh. Elektron.*, **56** (12), 1522 (2011).
7. Alekseev A.E., Tezadov Ya.A., Potapov V.T. *Kvantovaya Elektron.*, **42**, 76 (2012) [*Quantum Electron.*, **42**, 76 (2012)].
8. Alekseev A.E., Tezadov Ya.A., Potapov V.T. *Pis'ma Zh. Tekh. Fiz.*, **38** (24), 67 (2012).
9. Alekseev A.E., Tezadov Ya.A., Potapov V.T. *Radiotekh. Elektron.*, **58** (3), 292 (2013).
10. Goodman J.W. *Statistical Optics* (New York: Wiley–Interscience, 1985; Moscow: Mir, 1988).
11. Gysel P., Staubli R.K. *J. Lightwave Technol.*, **8** (4), 561 (1990).
12. Mandel L., Wolf E. *Optical Coherence and Quantum Optics* (Cambridge: Cambridge University Press, 1995; Moscow: Fizmatlit, 2000).
13. Tkach R., Chraplyvy A. *J. Lightwave Technol.*, **4** (11), 1711 (1986).
14. Salehi M.R., Cabon B. *J. Lightwave Technol.*, **22** (6), 1510 (2004).
15. Desurvire E. *Erbium-Doped Fiber Amplifiers, Principle and Applications* (New York: Wiley, 1994).